Small Scale Experimental Study of Vaporization Fluxes of Liquid Nitrogen Released on Water

Nirupama Gopalaswami and M. Sam Mannan, Mary Kay O'Connor Process Safety Center, Artie McFerrin Department of Chemical Engineering Department, Texas A&M University System, College Station, Texas 77843-3122, USA

Luc Vechot and Tomasz Olewski, Mary Kay O'Connor Process Safety Center – Qatar, Texas A&M University at Qatar, PO Box 23874, Doha, Qatar

One of the key steps in Liquefied Natural Gas (LNG) source term modeling is the characterization of heat transfer between substrate and cryogenic liquid. The boiling of cryogenic liquid on water exhibits an immiscible liquid-liquid heat transfer phenomenon where heat transfer parameters change rapidly in a short duration of time. The convective boiling of LNG on over water is influenced by different physical properties of the components present in LNG and the hydrodynamic phenomena that are influencing the boiling process. The boiling process starts on a film boiling regime owing to the large temperature difference and may transfer to transition and nucleate boiling regime as the temperature difference between water and cryogenic liquid decreases. A small scale experimental study was conducted using liquid nitrogen to investigate the heat transfer behavior of cryogenic liquids on water. The amounts of cryogenic spilled and initial water temperature were varied to determine their effect on vaporization rates. The vaporization rates were determined directly from the mass loss measured during the experiment. A variation of heat transfer rate was observed with the change of initial water temperature. The heat flux from water to liquid nitrogen was determined from experimental data and the correlation for convective boiling was validated. Liquid nitrogen was found to be predominantly in film boiling regime. Significant ice formation was observed in spills where the initial water temperature was low. Statistical performance measures were employed to test the performance of phenomenological model for predicting heat flux from water to liquid nitrogen. The model predictions were found to be within a factor of two of the observations. The validated heat flux prediction model is to serve as a sub-model for source term modeling of cryogenic liquid spills.

Keywords: Source term, Convective Boiling, Vaporization, Liquid Nitrogen, Experimental Measurement

Introduction

One of the most important factors which affect cryogenic release on water is the heat flux from water. The rate at which vapor is being generated in the event of an accidental spill of a cryogenic on water largely depends on the rate of heat transfer from water to cryogenic liquid. This rapid heat transfer rate to the cryogenic liquid pool is significantly affected by the temperature difference between water and cryogenic liquid.

Various research centers have performed experiments on cryogenic boiling on water Drake, Jeje and Reid (1975a),(Ali, Drake and Reid 1975), (Nakanishi & Reid, 1971),(D. Burgess, Murphy, & Zabetakis, 1970). In all these experiments the source term was calculated by measuring the heat flux through weight loss or temperature values of water. This was possible by measuring the temperature difference between the substrate and cryogenic pool and using analytical expressions to determine the heat flux. It is to be noted that most of these experiments were instantaneous in nature, lacking temperature data of bulk water for heat flux calculation. The results of small scale experiments are difficult to scale up as the water bulk in small confined space of the boiling cell is cooled off very quickly and thus vapor film breaks down quickly because the temperature difference is not enough to maintain a film boiling regime. Scaling up of these data to large scale releases of LNG involves analysis of factors that will reflect this issue. Theoretical correlations were also developed by many researchers and it is important to note that these were originally developed for boiling on solid surface and seems to under predict the heat flux values and hence the vaporization rates on water (Drake, Jeje, & Reid, 1975a)(Drake et al., 1975a). The shift of boiling regimes and its effect on vaporization rates is not clearly known. This will be discussed later in the paper.

In this work, the convective boiling model for transfer of heat from water to cryogenic liquid is investigated through small scale experiment. The study is performed to verify the boiling regimes of cryogenic liquids boiling on water and independently validate the vaporization model for cryogenic liquid boiling on water. Statistical performance measures were adopted to evaluate the performance of the model in predicting heat fluxes. The validated heat flux prediction model is to be used as a sub-model in a Computational Fluid Dynamics (CFD) model for pool spreading and vaporization.

Experimental Setup and Procedure

The experimental setup designed for small scale spills of liquid nitrogen on water is shown in Figure 1. The small scale experiments were performed in a wind tunnel build at the Fire Station 2 of the Ras Laffan Industrial City, Qatar. The wind tunnel was 12 m long (experimental setup was located in 8 m from inlet) and 2 m wide and 0.855 m tall offering a convenient space for

safe dispersal of vapor. The setup consists of a metallic cylinder with an inner diameter of 58.5 cm and a height 87.5 cm made of carbon steel. A stainless steel chimney without bottom and top with dimensions 35X35X80 cm was placed inside the metal cylinder to protect it from fractures resulting from cryogenic spill. The stainless steel chimney was square shape in cross-section and devoid of top and bottom. The square cross-sectional area was 0.1225 m^2. The stainless steel chimney was lowered into the metallic cylinder using a steel support in such a way that it is half filled with water at any point of time during the experiment and the liquid nitrogen was spilled inside the chimney. Such a setup protected cylinder from fractures at cryogenic temperatures. The setup also ensured that liquid nitrogen interacted only with stainless steel walls of chimney and water. The temperature of water, liquid nitrogen and nitrogen vapor was monitored by distributed N-type thermocouples. The thermocouples were mounted on two polycarbonate boards and each included sixteen thermocouples distributed vertically. One board was mounted near the wall of stainless steel box and the other was held in the center of the box. The polycarbonate board was suspended into the metallic cylinder in such a way that 11 thermocouples measured the temperature below water, three measured liquid nitrogen temperature and two measured liquid nitrogen vapor temperature. Each of these thermocouples was calibrated and the temperature was measured every second. The thermocouples were distributed with smaller distances near the water-liquid nitrogen surface. The cryogenic hose was placed in the middle of the setup to ensure smooth discharge of liquid nitrogen on water. The width of the tunnel was considered x axis and length of the wind tunnel was considered as the y axis. The entire setup is placed on a weighing balance (maximum load – 300 kg and sensitivity – 100 g) to note the change in mass when nitrogen is vaporizing on water. The sensors' output is recorded every second (1Hz) by a Data Acquisition system (DAQ), and the recorded data is sent to a computer for processing.

The cylinder was half filled with water before the start of the experiment. The liquid nitrogen was discharged continuously from a 180 liter capacity tank through a cryogenic hose of length 15 m and internal diameter 0.0127 m. The mass of the all setup was recorded every 1 second and was used to measure the LN2 vaporization rate. The time for opening/closing the cryogenic valve and the time when liquid nitrogen touched water was noted. The time of discharge and the mass increasing in the box were recorded, and the rate of liquid discharge was calculated based on these data with the assumption that the flashing of LN2 in the air is neglected. Such defined release rate during each spill was calculated and is given in Table 1. After completion of each experimental run (when liquid nitrogen completely vaporized), the ice thickness (if formed) was estimated and the water was stirred to uniform temperature and final bulk temperature was measured. The experiment was repeated five times with different amounts of liquid nitrogen. A summary of the five experimental runs with some key-parameters is given in Table 1.

Table 1. Summary of experiments

Run Number	Amount Spilled (kg)	Release Rate ($kg\ s^{-1}$)	Initial Water Temperature (℃)	Vaporization Rate ($kg\ m^{-2}s^{-1}$)	Estimated Heat Flux to the pool ($kW\ m^{-2}$)
Run 1	4.7	0.07	45	0.31±0.06	62.3
Run 2	9.4	0.05	40	0.33±0.05	66.0
Run 3	9.8	0.03	31	0.34±0.05	68.1
Run 4	9.0	0.03	13	0.22±0.08	49.8
Run 5	14.6	0.13	41	0.39±0.09	78.5

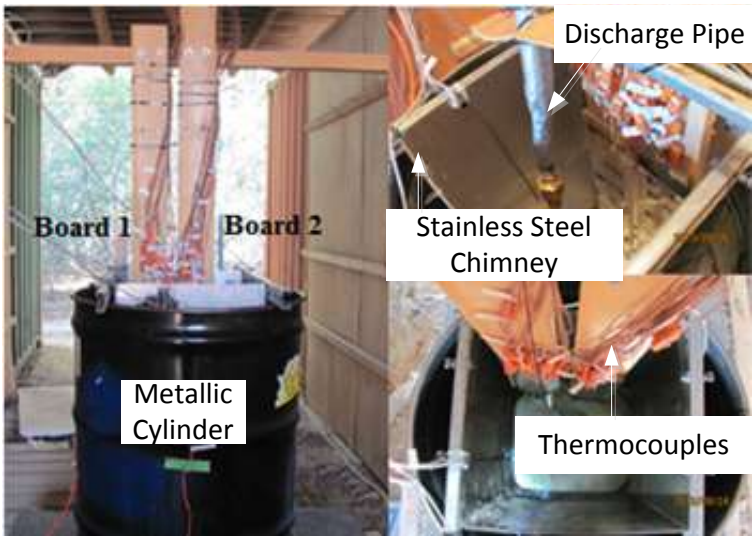

Figure 1. Top and lateral views of experiment

Convective Boiling Model

A boiling of cryogenic liquid spilled on water can be modeled by the convective boiling model, which involves the dynamic determination of heat transfer from the bulk of water to the cryogenic liquid pool as the function of the heat transfer coefficient and the temperature difference between water and the cryogenic liquid. When a cryogenic liquid touches the water surface, a large temperature difference exists between these two immiscible liquids and this result in rapid boiling with a formation of vapor film between cryogen and water surface leading to film boiling. When the water temperature decrease with time, the temperature difference between the two liquids reduces. As a result of this, the film boiling regime may shift to transition regime and to nucleate boiling when the spill area is small. The boiling regimes pattern is usually expressed as a Nukiyama curve which shows the wall superheat in horizontal axis and heat flux on the vertical axis (see Figure 2). Two critical points are observed in such a behavior to characterize the shift in boiling regimes, namely the Leidenfrost point and Critical Heat Flux (CHF) point. The film boiling occurs above the Leidenfrost point, whereas the nucleate boiling occurs below the Critical Heat Flux (CHF) point. Any temperature difference between these two points results in transition boiling.

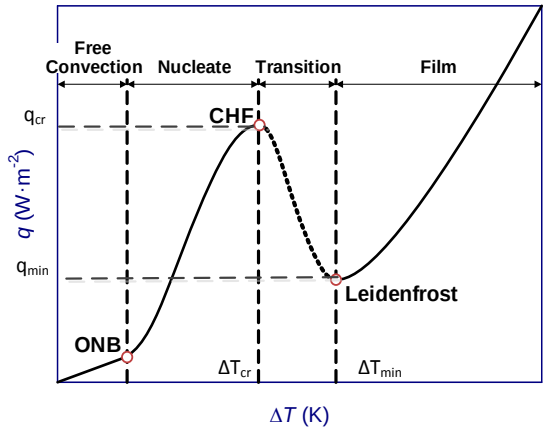

Figure 2: Boiling Curve

Based on the temperature differences, the boiling regimes can be determined. Substantial theoretical correlations exist for predicting the heat flux produced in each regime and the one developed by (Kalinin, Berlin, Kostyuk, & Nosova, 1976) is applied here with an exception for film boiling heat transfer coefficient. The film boiling heat transfer coefficient applied here was developed by Berenson (1960) and thus the film boiling heat flux is given as

$$q_f = \mathrm{h_f} * \Delta T = 0.425 \left[\frac{k_V^3 \lambda \rho_V (\rho_L - \rho_V)}{\mu_V \Delta T \left(\frac{g(\rho_L - \rho_V)}{\sigma} \right)^{\frac{1}{2}}} \right]^{\left(\frac{1}{4}\right)} * \Delta T \quad \text{Given if} \quad \Delta T > \Delta T_{min} \tag{1}$$

Nucleate Boiling is given by Kalinin et Al (Kalinin et al., 1976)

$$q_n = \frac{4.1 \left[1 + 10 \left(1 - \frac{\rho_v}{\rho_l} \right)^{\frac{2}{3}} \right] \Delta T^3}{\sigma T_s \left[\frac{\nu_l}{k_l} + \frac{10}{\sqrt{\rho_w c_{p_w} k_w}} \right]^2 \left(1 + \frac{10}{\gamma} \right)} \quad \text{If } \Delta T < \Delta T_{cr} \tag{2}$$

Transition Boiling is given by Kalinin et Al (Kalinin et al., 1976)

$$q_t = q_n \epsilon + q_f (1 - \epsilon) \quad \text{If } \Delta T_{cr} < \Delta T < \Delta T_{min} \tag{3}$$

To calculate the parameter ϵ a dimensionless temperature is introduced written as

$$\Delta T^* = \frac{\Delta T - \Delta T_{cr}}{\Delta T_{min} - \Delta T_{cr}} \tag{4}$$

$$\epsilon = (1 - \Delta T^*)^7 \tag{5}$$

Where wall superheat at Leidenfrost point ΔT_{min} Kalinin et Al (Kalinin et al., 1976)

$$\Delta T_{min} = (T_c - T) * \left[0.16 + 2.4\left(\frac{\rho_L C_{P_L} k_L}{\rho_w C_{p_w} k_w}\right)^{\left(\frac{1}{4}\right)}\right] \quad (6)$$

The minimum heat flux associated with Leidenfrost Point is given by (Forster & Zuber, 1955)

$$q_{min} = 0.177\ \Delta H_v \rho_v \left[\frac{\sigma g(\rho_l - \rho_v)}{(\rho_l + \rho_v)^2}\right]^{\frac{1}{4}} \quad (7)$$

The critical temperature difference is given by and critical point ΔT_{cr}

$$\text{And } \Delta T_{cr} = \frac{0.625[q_{cr}\sigma T]^{\frac{1}{3}}.\left[\frac{10}{\rho_w c_w k_w} + \frac{\sqrt{\frac{\mu_L}{\rho_L}}}{K_L}\right]^{\frac{2}{3}}\left[1+10\sqrt{\frac{\rho_L c_L k_L}{\rho_w c_w k_w}}\right]^{\frac{1}{3}}}{1+10\left(\frac{\rho_{VF}}{\rho_L - \rho_{VF}}\right)^{\frac{2}{3}}} \quad (8)$$

The peak nucleate heat flux is given by Kutateladze formulation (Kutateladze, 1961)

$$q_{cr} = 0.168\ \Delta H_v [\sigma g_c(\rho_L - \rho_V)]^{\frac{1}{4}}\sqrt{\rho_V} \quad (9)$$

An algorithm to determine the heat flux from water at particular temperature to cryogenic liquid pool is given below

- Calculate boiling parameters: ΔT_{min} , q_{min} at Leidenfrost point and ΔT_{cr}, q_{cr} at critical point from cryogen & water properties (Eqn. 6,7,8 and 9).
- Determine the temperature difference ΔT between water and cryogen from the thermocouples placed in water. ΔT , the wall superheat is the temperature difference between water temperature and LNG boiling point.
- If $\Delta T > \Delta T_{min}$, Calculate the film boiling heat flux (first row in Eqn. 1)
- If $\Delta T_{cr} < \Delta T < \Delta T_{min}$ Calculate the transition boiling heat flux (Eqn. 3, 4 and 5)
- If $\Delta T < \Delta T_{cr}$, Calculate the nucleate boiling heat flux (Eqn. 2)

The algorithm is summarized as

$$q = \begin{Bmatrix} q_{film} = h_{film}\Delta T & \Delta T > \Delta T_{min} \\ q_{nucleate} & \Delta T < \Delta T_{cr} \\ q_{transistion} & \Delta T_{cr} < \Delta T < \Delta T_{min} \end{Bmatrix} \quad (10)$$

Results and discussion

The results of small scale experiments are discussed in sections 4.1, 4.2 and the validation of model with experimental data is given in section 4.3 and 4.4.

Vaporization flux

The mass flux of vapor was determined from mass loss data obtained during the experiment. An averaging time of 30 seconds was used to compute the vaporization rates of the liquid nitrogen on water. The spill area included the constant cross sectional area of contact with water surface (0.138 m^2) and a variable area based on the height of the liquid nitrogen interacting with stainless steel walls. The average area based on the height of liquid varied from 0.01 to 0.09 m^2. Initially the amount of vapor produced is high as the temperature difference between liquid nitrogen and water is high. As water cools down, the temperature difference between liquid nitrogen and water reduces and heat transfer to the pool also reduces. The heat flux is also restricted by the growing ice film in the pool which offers resistance to heat transfer. The vapor mass flux showed a decreasing trend in all experimental runs where the initial water temperature was high. When the initial water temperature is high, the heat transfer from water to the liquid nitrogen occurs through convection mechanism *i.e.* the water surface which is cooled by liquid nitrogen is replenished by the hot water from the bulk to the surface. This convective heat transfer is restricted completely when a thick ice sheet is formed in the cases where water temperature is low. When the initial water temperature is low, heat transfer to the cryogen is restricted by the growing ice sheet which does not allow hot bulk to be replaced at the surface. This trend is observed in tests where the initial water temperature was 13˚C and 31˚C, where a constant vaporization rate was observed. The 30 s averaged vaporization rates for each run are showed in Figure 3. The range of vaporization rate observed at each test and the heat flux are summarized in Table 1. For example, an average vaporization flux of 0.33 kg $m^{-2}s^{-}1$ was observed in the run 3, which

represent an average heat flux of 65 kW m^{-2}. The vaporization flux of liquid nitrogen was not sensitive to the amount spilled. However, as expected, the initial vaporization rates were dependent on the initial water temperature and spill rate. The vaporization rates obtained in this experiment expressed good agreement with data obtained by Bureau of Mines (D. Burgess, Biordi, & Murphy, 1972) but is not in agreement with data obtained by Drake et Al (1975a).This might have been due to the variation in spill area observed in these tests.

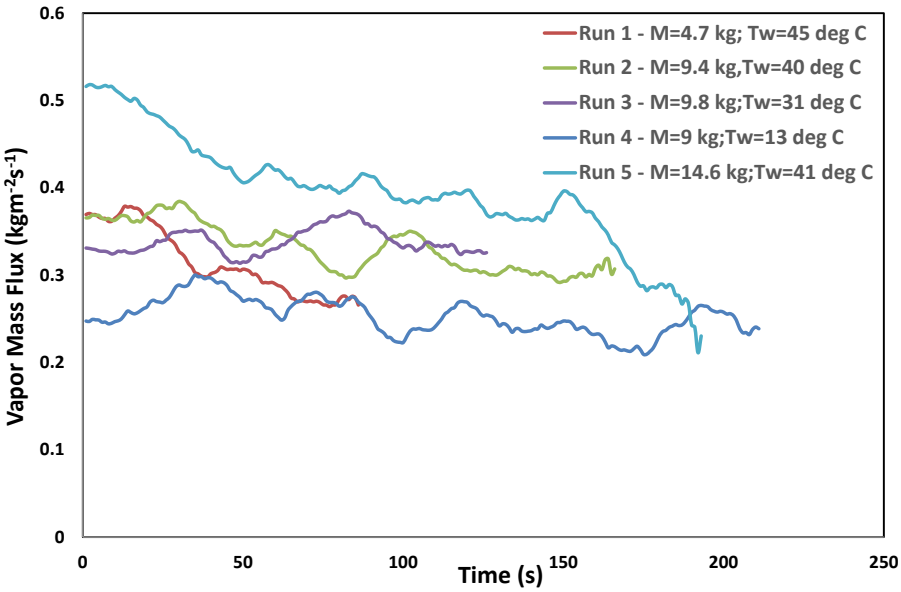

Figure 3: Vaporization flux

Temperature profiles below water surface

One of the significant features of a release of liquid nitrogen on water is the immersion of cryogenic liquid into water due to density difference. This phenomenon is important in determining the pool height of liquid nitrogen and its effect of vaporization. However, in small confined releases, the pool height is restricted by the boundaries of the confined area and would constitute a significant head of liquid nitrogen. This liquid head will reduce along with vaporization if the liquid nitrogen.

Figure 4 shows the temperature values at various levels below water for run 1. The figure also shows the change in mass with time during the spill as dashed black line. As LN2 mass was continuously added to the setup, the thermocouples contacted liquid nitrogen and it reflected its temperature. This is observed in thermocouples placed at 0.25 cm and 0.75 cm below the water surface. When the temperature difference between LN2 and water was high (~200 – 100 K), film boiling was found to be dominating and as this temperature difference dropped to a value less than 70 K, transition boiling was observed. Such low temperature differences were momentary and were present in test during the end of vaporization. The heat fluxes obtained were 1.5 times as much as the average heat flux in each test.

As liquid nitrogen is added to the stainless steel box, the liquid nitrogen immerses into water and displaces an equivalent amount of water outside the cover. This immersion of liquid nitrogen in water can be seen effectively from the values of thermocouples placed at distances 0.25, 0.75 and 1.3 cm below water. The immersion height (immersed head) of liquid nitrogen below water can be calculated through a simple mass balance in the system containing water and liquid nitrogen and is given by

$$h_{im} = \left(\frac{m_L}{\rho_W A_W}\right).\frac{(A_W - A_L)}{A_L} \quad (11)$$

where h_{im} is the head of liquid nitrogen below water

m_L is the mass of liquid nitrogen spilled,

A_w is the cross sectional area of cylinder

A_L is the cross sectional area of the steel walls box (box)

The head of liquid nitrogen above water was calculated by subtracting the total head of liquid nitrogen from the immersed head. Table 3 provides a value of immersion height of liquid nitrogen below water and head liquid nitrogen above water. From the values, it can be seen that about 45% of the liquid nitrogen gets immersed into water in each test.

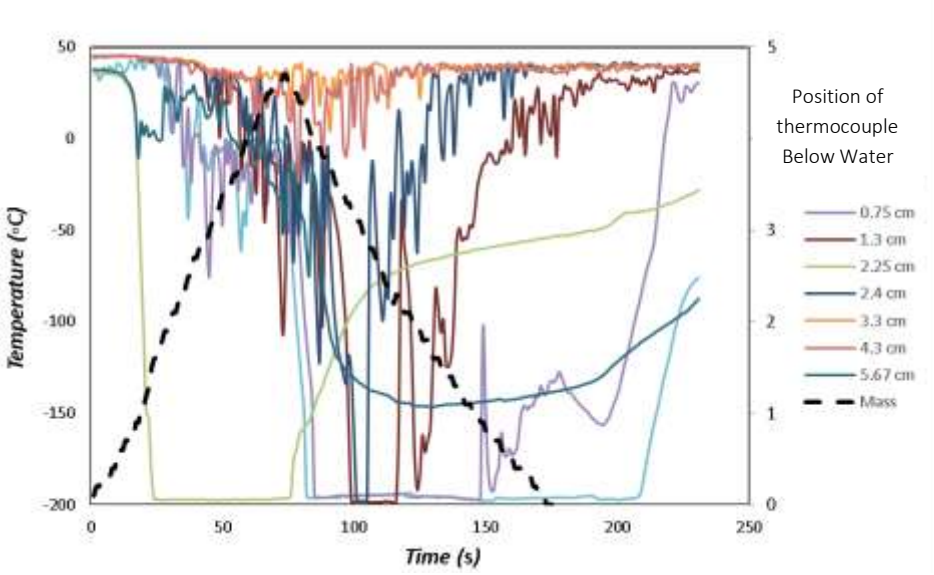

Figure 4: Temperature profiles of thermocouple below water surface

Table 2: Height of liquid nitrogen below and above water

h_{im} (cm)	H_{ab} (cm)
2.09	2.61
4.18	5.22
4.35	5.45
4.00	5.00
6.49	8.11

Thermocouples placed deeper than 6 cm below the water surface registered very low change in temperature and they represented the bulk water temperature for the entire experiment duration (not shown in the figures here). This observation may indicate that all temperature gradient in water happen within about 6 cm thick layer near the cryogenic pool and bulk water can be assumed to be at uniform temperature.

It is to be noted that the thermocouple which was placed 2.25 cm below water surface dropped down to cryogenic temperatures during the spill. This can be explained by the penetration of liquid nitrogen jet and currents into the water, which contacted this thermocouple.

Comparison of experimental and theoretical heat flux

A comparison of heat flux predicted by the model with the heat flux obtained in the experiment (section 4.1) was performed. The heat flux from was calculated using the correlations discusses in section 3 of this paper. The temperature values recorded during the experiment were used in these calculations. Performance statistics were applied here to evaluate the performance of the theoretical model for predicted heat fluxes. Applied statistics were initially recommended by Fox, (1984) and applied by (Hanna, Chang, & Strimaitis, 1993). The statistical performance measures include the fractional bias (FB), the geometric mean bias (MG), the normalized mean square error (NMSE), geometric variance and fraction of predictions within a factor of two of observed experimental data (FAC2). The correlations for each statistical measure are given below.

$$\text{Geometric Mean Bias, MG} = \exp\left(\overline{\ln\left(\frac{C_m}{C_p}\right)}\right) \quad (6)$$

$$\text{Geometric Variance, VG} = \exp\left(\overline{\ln\left(\frac{C_m}{C_p}\right)}\right)^2 \quad (7)$$

$$\text{Fractional Bias, FB} = \frac{(\overline{C_m}-\overline{C_p})}{0.5\,(\overline{C_m}+\overline{C_p})} \quad (8)$$

$$\text{Normalized Mean Square Error} = \frac{\left(\overline{C_m} - \overline{C_p}\right)^2}{\overline{C_m}.\overline{C_p}} \quad (9)$$

$$\text{Factor of two FAC2} = C_p/C_m \quad (10)$$

Where C_m is an experimental value of the heat flux provided from water to the cryogenic liquid pool, and $C_p$is the model prediction.

The factor of two (FAC2) is a fraction of data that satisfies $0.5 \leq C_p/C_m \leq 2$, where C_p is the Model prediction and C_o experimental value. A perfect model is bound to have MG, VG and FAC2=1, FB and NMSE=0. However, the model is bound to display a small error if the variability in model solutions is equally compensated by the natural variability occurring in the experiment. However this variability in measured and model predictions arise from different sources. The variability in observations can be attributed to flashing that takes place during discharge and fluctuations due to penetration of a liquid nitrogen jet into water, whereas the variability in model can be due to input data or model physics errors. To account for such variations and establish the performance of model prediction, the factor of 2 is widely used. According to this statistical performance measure, a model is deemed to be good if the majority of the solutions fall within a factor of 2 (± 33%) of the observations. The measured and predicted heat fluxes are discussed here owing to its importance in source term modelling. A comparison of theoretical and experimental values of heat flux is shown in Figure 5. The scatter plot is drawn for a total of 250 points where all predicted and experimental heat fluxes have been paired up in space. A total of 50 data points from each test are used to plot the FAC2 plot. Multiple statistical performance measures are calculated simultaneously here as each has its own advantages and disadvantages based on the range of model predictions and measured values.

Bias is basically the mean difference between predicted and measured values. Fractional bias is normalized form of Mean Bias to make it non-dimensionless. This fractional bias (FB) varies between +2 (extreme over prediction) and -2 (Extreme under prediction) and has an ideal model has a value of 0. Positive FB values represent over-prediction and negative FB values represent under prediction. Geometric mean bias (MG) is the logarithmic form of bias. An ideal model will have value 1. An MG greater than 1 implies that the model overestimates and an MG less than 1 that the model underestimates. Normalized mean square error (NMSE) emphasizes the scatter in the entire data set. A value of NMSE=1 implies that root mean square error is equal to the mean and values of NMSE>1 implies that the distribution is closer to log normal than normal. A good model has NMSE value 0. Geometric mean variance (VG) expresses the scatter of log-normal distribution. It is usually used range of measured values evaluated is wide. An ideal model will have VG= 1.Typical values of model acceptance criteria are required to claim a model to be good in predicting heat fluxes. To test the ability of a mathematical model in the current study, the following acceptance criteria are used. The fraction of predictions within a factor of two observations is 50% (FAC2>50%). The mean bias is within ± 30% of the mean (*i.e.* -0.3<FB<0.3 or 0.7<MG<1.3). The random scatter is about a factor of two of the mean (i.e. NMSE<4 or VG <1.6).

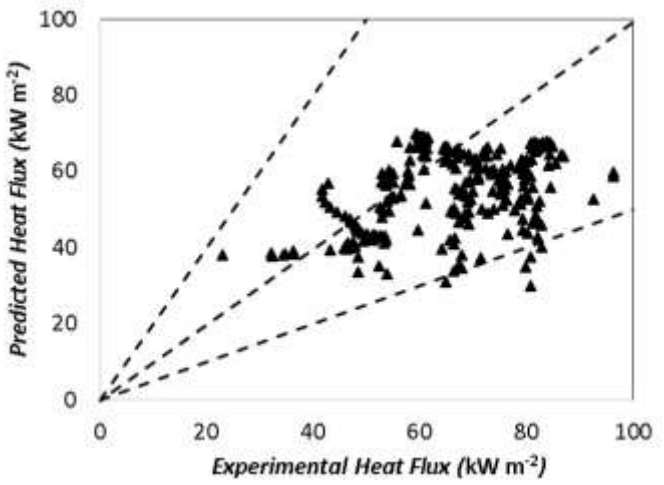

Figure 6 Comparison of Predicted and Experimental Values of Heat Flux

Table 3: Statistical performance measure for all the experimental runs

Max C_m	Max C_p	Mean C_m	Mean C_p	FAC2	MG	VG	FB	NMSE
67.87	69.38	66.05	70.26	0.98	1.06	1.04	0.03	0.04

The statistical performance measures for all data points are given in Table 3. A positive fractional Bias of values closer to zero was obtained implying a mean over prediction. The FAC2 value was found to be 0.98 implying that 98% of the predictions were within a factor of two of the observations. The geometric mean, MG, is a ratio of geometric mean of measured value to the geometric mean of predicted value and has a value of 1.06 in this study implying that the mean bias was within ± 30% of the mean. A VG value of 1.04 represents that the scatter is less than 50% of the mean. A FB and mean$\frac{C_p}{C_m}$ implies an under prediction of model by 3%. The NMSE value of 0.04, which is less than 4, is a measure of the mean relative scatter.

Boiling regimes

A boiling curve was developed to determine the boiling regimes of the liquid nitrogen boiling on water (discussed in section 0). The Leidenfrost point, which determines the temperature boundary between film and transition boiling, was calculated to be 75.8 K. Similarly, the critical heat flux (CHF) point, the temperature boundary between nucleate and transition boiling, was found to be 2.2 K. Estimated wall superheat values and corresponding experimental heat fluxes are shown in (Figure 7). The heat flux data obtained in all experimental runs represent the heat flux of film boiling and the transition or nucleate boiling were not observed. It can be seen that experimental data show rather constant vaporization rate over duration of each test. Observed vaporization rates (heat flux) is well represented by the model when the temperature difference between water and LN_2 is high (beginning of the spill) and accuracy decreases when temperature difference decreases. Obviously, larger reduction in temperature difference occurs when larger amount of liquid nitrogen is spilled (not shown in tables). The largest temperature reduction was observed in run 5 where 14.6 kg of liquid nitrogen was spilled (Table 1).

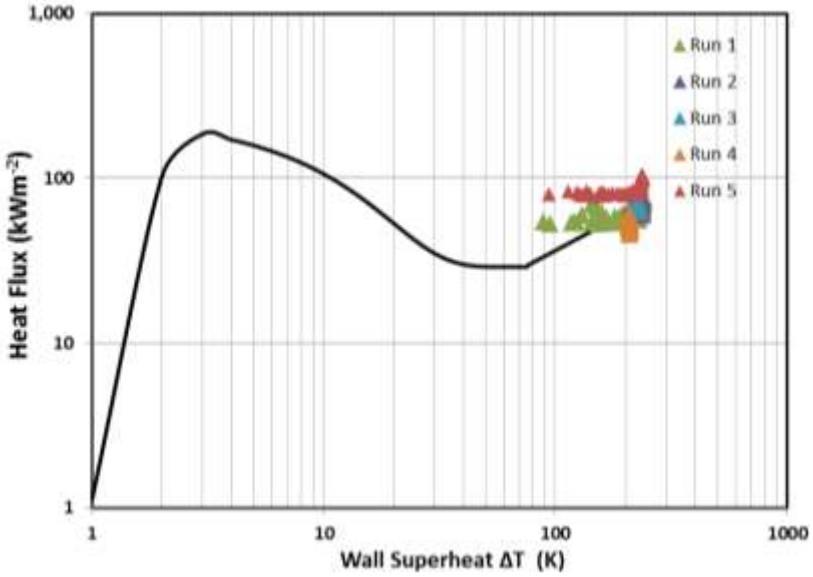

Figure 7 Boiling regimes of liquid Nitrogen released on water

Ice formation

The confined releases have been associated with significant ice formations. In run 1, run 2 and run 5, when initial water temperature was more than 40˚C, no ice formation was observed. When the initial temperature was 31˚C (run 3), ice was found deposited on the walls of the setup and polycarbonate board. The ice formed in run 3 was powdery and melted quickly. When the initial temperature was reduced further to 13˚C (run 4) an ice sheet of thickness 6.5 ± 0.5 cm was formed. The ice formed was smooth and opaque in nature (see Figure 7).

Figure 7: Ice formation in Run 3 (left) and Run 4 (right)

Conclusion

An experimental investigation of small scale continuous releases of liquid nitrogen on water was performed to improve the understanding of source term modelling of cryogenic liquid spills. The vaporization rates obtained were independent of the amount of liquid nitrogen spilled and the release rate. A variation in heat transfer mechanism was observed with changes in initial water temperature. Significant ice formations were observed in spills where the initial water temperature was low. An average of 45% of the liquid nitrogen head was found immersed into water. The temperature of liquid nitrogen pool was found stable and equal to its boiling point. The bulk water temperature remained the same during the experiments. The performance of the model in predicting heat fluxes was found to be good as 98% of the predictions are within a factor of two of the observations. An under-prediction of about 3% was observed from the values of FB for the model. The geometric mean bias was 6% from the perspective value and the random scatter was very low indicating that their scatter is approximately equal to the mean. The validated heat flux prediction model is to be used as a sub-model in a Computational Fluid Dynamics (CFD) model for pool spreading and vaporization.

Acknowledgements

The authors would like to thank BP Global Gas SPU for their financial support and guidance. They would also like to acknowledge the support of Qatar Petroleum (QP) for offering facilities at Ras Laffan Industrial City. The authors personally thank QP's staff who worked with LNG research team of Texas A&M University at Qatar for great support provided, which exceed the authors' expectations.

References

Ali, D. K., Drake, E. M., & Reid, R. C. (1975). Boiling of liquid Nitrogen and Methane on water. The effect of Initial Water Temperature. *International Journal of Heat and Mass Transfer*, *31*(2), 176–177.

Berenson, P. J. (1960). Transition Boiling Heat Transfer from a horizontal surface.

Burgess, D. ., Murphy, J. ., & Zabetakis, M. . (1970). *Hazards of LNG spillage in marine transportation* (p. 70). Pittsburgh, Pennsylvania.

Burgess, D., Biordi, J., & Murphy, J. (1972). *Hazards of spillage of LNG into water* (p. 93). Pittsburg, Pennslyvania.

Drake, E. M., Jeje, A. a., & Reid, R. C. (1975a). Transient boiling of liquefied cryogens on a water surface. *International Journal of Heat and Mass Transfer*, *18*(12), 1361–1368. doi:10.1016/0017-9310(75)90249-5

Drake, E. M., Jeje, A. A., & Reid, R. C. (1975b). Transient Boiling of Liquefied Cryogens on a water surface. *International Journal of Heat and Mass Transfer*, *18*(12), 1369–1375.

Forster, H. K., & Zuber, N. (1955). Dynamics of Vapor Bubbles and Boiling Heat Transfer. *AIChE Annual Meeting*, *1*(4), 531–535.

Fox, D. . (1984). Uncertainity in air quality modeling. *Bulletin of the American Meteorological Society*, *65*, 27–36.

Hanna, S., Chang, J., & Strimaitis, D. (1993). Hazardous gas model evaluation with field observations. *Atmospheric Environment. Part A. …*, *27*(15). Retrieved from http://www.sciencedirect.com/science/article/pii/096016869390397H

Kalinin, E. K., Berlin, I. I., Kostyuk, V. V, & Nosova, E. M. (1976). Heat transfer in transition boiling of cryogenic liquids. *Advances in Cryogenic Engineering*, *21*, 273–277.

Kutateladze, S. S. (1961). Boiling heat transfer. *International Journal of Heat and Mass Transfer*, *4*, 31–45.

Nakanishi, E., & Reid, R. C. (1971). Liquefied Natural Gas-Water Reactions. *Chemical Engineering Progress*, *67*(12), 36–41.

Nomenclature

Cp	Specific heat Capacity (J $kg^{-1}K^{-1}$)
g	Acceleration due to gravity (m s^{-2})
Hv	Latent Heat of vaporization (J kg^{-1})
k	Thermal Conductivity (W $m^{-1}K^{-1}$)
q	Heat flux (W m^{-2})
T	Temperature (K)

Greek Letters

ε	Constant in transition boiling
μ	Viscosity (kg $m^{-1}s^{-1}$)
ρ	Density (kg m^{-3})
σ	Surface Tension (N m^{-1})

Subscripts

c	Critical Temperature
Cr	Maximum value at Critical Heat Flux (CHF) point for nucleate boiling
L	Liquid phase
min	Minimum
v	Vapor phase
vf	Vapor film
w	Water
s	Saturated